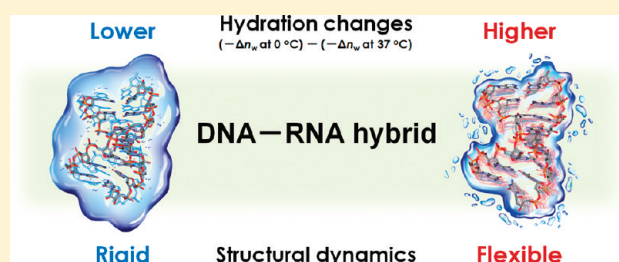


Conformational Flexibility Influences Degree of Hydration of Nucleic Acid Hybrids

Smritimoy Pramanik,[†] Satoru Nagatoishi,[†] Sarika Saxena,[†] Jhimli Bhattacharyya,[†] and Naoki Sugimoto^{*,†,‡}[†]Frontier Institute for Biomolecular Engineering Research (FIBER) and [‡]Faculty of Frontiers of Innovative Research in Science and Technology (FIRST), Konan University, 7-1-20 Minatojima-minamimachi, Chuo-ku, Kobe 650-0047, Japan**S** Supporting Information

ABSTRACT: Four nucleic acid duplexes—DNA/RNA hybrid, RNA/DNA hybrid, RNA duplex, and DNA duplex—were studied under molecular crowding conditions of osmolytes. Destabilization of duplexes ($\Delta\Delta G^{\circ}_{25}$) indicated that the $\Delta\Delta G^{\circ}_{25}$ values of hybrids were intermediate between those of DNA and RNA duplexes. In the presence of polyethylene glycol 200, the $\Delta\Delta G^{\circ}_{25}$ values were estimated to be +3.0, +3.5, +3.5, and +4.1 kcal mol⁻¹ for the DNA duplex, DNA/RNA hybrid, RNA/DNA hybrid, and RNA duplex, respectively. Differences in the number of water molecules taken up ($-\Delta n_w$) upon duplex formations between 0 and 37 °C ($\Delta(-\Delta n_w)$) were estimated to be 44.8 and 59.7 per duplex structure for the DNA/RNA and RNA/DNA hybrids, respectively. While the $\Delta(-\Delta n_w)$ value for the DNA/RNA hybrid was intermediate between those of the DNA (26.1) and RNA (59.2) duplexes, the value for RNA/DNA hybrid was close to that of RNA duplex. These differences in the thermodynamic parameters and hydration are probably a consequence of the enhanced global flexibility of the RNA/DNA hybrid structure relative to the DNA/RNA hybrid structure observed in molecular dynamics simulations. This molecular crowding study provides information not only on hydration but also on the flexibility of the conformation of nucleic acid duplexes.



INTRODUCTION

Nucleic acids play pivotal roles not only in genetic information storage but also in various biological functions. Therefore, the structure, stability, and function of RNA and DNA in living cells are of interest in the medical, pharmaceutical, biological, chemical, biophysical, and material sciences fields. The stability of nucleic acid structures depends on the balance of interactions among several factors, including base pairing and electrostatic interactions, and is sensitive to the environment. In particular, hydration impacts the structure and function of nucleic acids,^{1,2} and the so-called molecular crowding conditions related to osmotic pressure in living cells influence nucleic acid structure.³ Cells experience a variety of environmental stresses that reduce or increase the amount of intracellular water. To overcome the water stresses, organisms accumulate low molecular weight compounds called osmolytes or osmoprotectants that allow the organism to maintain cellular processes even under stress conditions.^{4,5} Among biologically relevant osmoprotectants, trimethylglycine and proline can be present at up to 1 M internal concentration in living cells.^{6–11} Several groups have studied the thermodynamics of DNA duplex formation in the presence of osmolytes such as trimethylglycine and proline.^{12–15} We have also reported that DNA duplexes are destabilized in the presence of zwitterionic cosolutes.¹⁶ Moreover, we have shown that the neutral osmolyte polyethylene glycol 200 (PEG 200) decreases the thermodynamic stability of nucleic acid structures.^{17–19} It is known that Watson–Crick and Hoogsteen base pair formations

are associated with hydration and dehydration, respectively.¹⁹ For example, the DNA duplex d(GAGGTCGT)/d(ACGACCTC) is destabilized upon duplex formation in PEG 200 than in buffer alone due to low water activity.²⁰

Helical structures of DNA and RNA are well characterized.²¹ Although it is clear that the structures of hybrids consisting of a DNA strand and an RNA strand are not a simple average of those of pure DNA and RNA duplexes, the helical conformations, thermodynamic stabilities, and structural flexibilities of the hybrids have been studied extensively with often contradictory results.^{22–30} We also previously reported sequence-dependent thermodynamics and nearest-neighbor parameters of the hybrid formation.^{31–36} The nature of hybrids depends on the base sequence and the solvent conditions. Hybrids are formed during the replication of cellular DNA and, hence, are important structures during gene expression.^{37,38} Hybrids are also intermediates in the synthesis of DNA in retrovirus replication and also occur in Okazaki fragments.^{39,40} Hence the characterization of hybrids is important to elucidate the biological functions.

The conformational flexibility of nucleic acids^{41–43} and non-canonical conformational transitions^{44,45} have been shown to have fundamental roles in biology. DNA duplex dynamics impact recognition by proteins,^{42,46–49} nucleosome positioning,⁴² and

Received: August 16, 2011

Revised: September 15, 2011

Published: October 12, 2011

formation of loops and other large-scale architectures in genomic DNA.⁵⁰ Recent *in silico* studies suggest that dynamics of duplex conformations are closely related with the hydration properties in duplex structures.^{51–54} An *in vitro* study of the correlation between conformational dynamics and hydration has a potential to clearly reveal the biological significance of duplex dynamics.⁴⁶ We showed recently that the thermodynamic stability of the hybrid can regulate the telomerase activity.⁵⁵ Thus, quantitative thermodynamic data on hybrid duplexes and an analysis of the correlation between structural dynamics and hydration properties are required in order to elucidate their role in biology and biotechnology.

In the present study, we investigated the effect of the osmolytes PEG 200, proline, and trimethylglycine on the thermodynamic stability of the DNA/RNA hybrid d(GAGGTCGT)/r(ACGACCUC), the RNA/DNA hybrid r(GAGGUCGU)/d(ACGACCTC), and corresponding RNA and DNA duplexes. These duplexes have the same sequence but different strand compositions. It is important to note that under the experimental conditions in this study, each duplex clearly gives two state transitions during melting, which is essential for accurate evaluation of thermodynamic parameters. The hybrid structures were destabilized in the presence of the osmolytes, and the effect appeared to be due to decreased water activity. Importantly, our present results suggested that the effect of the osmolytes on the thermodynamics of the hybrids depended on their helical conformation. The hydration states and the global helix flexibilities of the nucleic acid duplexes inferred from molecular dynamics (MD) simulations were correlated. The use of molecular crowding agents provided correlation between two important properties of nucleic acid duplexes that are the hydration status and the helical conformation.

MATERIALS AND METHODS

Oligonucleotides and Chemicals. DNA and RNA oligonucleotides purified by high-performance liquid chromatography were procured from Hokkaido System Science. Concentrations of the oligonucleotides were determined by measuring the absorbance at 260 nm at 90 °C using a Shimadzu 1700 spectrophotometer connected to a thermoprogrammer. Single-strand extinction coefficients were calculated from mononucleotide and dinucleotide data using the nearest-neighbor approximation.^{56,57} Osmolytes, betaine (trimethylglycine), and proline were Sigma products. PEG 200, NaCl, and sodium phosphate were obtained from Wako Chemicals. Disodium ethylenediaminetetraacetic acid (Na₂EDTA) was purchased from Alfa Aesar.

Circular Dichroism (CD) Measurements. CD experiments were performed on a JASCO J-820 spectropolarimeter at 4 °C in a 1.0-mm path length quartz cuvette at a total strand concentration of 20 μM in a buffer containing 10 mM sodium phosphate (pH 7.0), 1 M NaCl, and 1 mM Na₂EDTA with or without osmolyte. The CD spectrum was the average of at least three scans measured from 200 to 350 nm at a scan rate of 100 nm min^{−1}. The temperature of the cell holder was regulated by a JASCO PTC-348 temperature controller, and the cuvette-holding chamber was flushed with a constant stream of dry nitrogen gas to avoid condensation of water on the cuvette exterior. Before measurement, the sample was heated to 80 °C, cooled at a rate of 1 °C min^{−1}, and incubated at 4 °C for 1 h.

Thermodynamic Analysis. UV absorbances of different samples were recorded in a Shimadzu 1700 spectrophotometer

equipped with a temperature controller. Melting curves of nucleic acid structures were obtained by measuring the UV absorbance of samples in either a 1-cm or a 1-mm path length quartz cell at 260 nm in a buffer containing 10 mM sodium phosphate (pH 7.0), 1 M NaCl, and 1 mM Na₂EDTA with or without osmolyte. At low temperature, the water condensation on the cell exterior was avoided by a constant stream of dry nitrogen. Thermal denaturation and renaturation of all the duplex structures were measured both in the absence and in the presence of osmolytes. The heating and cooling rates were 0.5 °C min^{−1}. It is important to note that under all conditions, denaturation and renaturation profiles were identical as assessed by measuring UV absorbance at 260 nm. This lack of hysteresis indicates that the transition between single strand and duplex is two state. The T_m values for the hybrid and duplex structures were obtained from the UV melting curves as described previously.¹⁸ Thermodynamic parameters were obtained from the UV melting curves using the following equation:³²

$$T_m^{-1} = [R \ln(C_t/4) + \Delta S^\circ]/\Delta H^\circ \quad (1)$$

where ΔS° and ΔH° are calculated entropy and enthalpy changes for the duplex formation, respectively, R is the gas constant, and C_t is the total strand concentration. The free energy change at 25 °C (ΔG°_{25}) was evaluated using the following equation:

$$\Delta G^\circ_{25} = \Delta H^\circ - T\Delta S^\circ \quad (2)$$

where $T = 298.15$ K (25 °C). Before measurement, the samples were heated to 80 °C, cooled at a rate of 1 °C min^{−1}, and incubated at 0 °C for 1 h to remove any nonequilibrium structures.

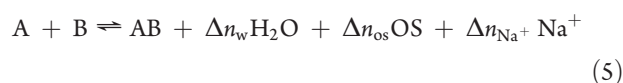
Water Activity Measurements. The water activities were determined via vapor phase osmometry using a model 5520XR pressure osmometer (Wescor). The water activity (a_w) was estimated from the measured osmolality (mmol kg^{−1}) using the following equation:⁵⁸

$$\Psi = (RT/M_w) \ln a_w \quad (3)$$

where Ψ and M_w represent the water potential and the molecular weight of water (0.018 kg mol^{−1}), respectively, R is the gas constant, and T is the temperature in Kelvin. The relationship between water potential and osmolality, assuming independence of the water potential on temperature at room temperature, is given by the equation⁵⁸

$$\Psi(\text{MPa}) = \text{osmolality}(\text{mmol kg}^{-1}) \times 10^3 / (-400) \quad (4)$$

Intermolecular duplex formation by two single strands (A and B) in an aqueous solution containing osmolyte (OS) and sodium ion (Na⁺) can be represented by the following reaction:



where, Δn_w , Δn_{os} , and Δn_{Na^+} are the numbers of water molecules, osmolyte, and sodium ions released upon the duplex (AB) formation, respectively. At a fixed temperature and pressure, the observed equilibrium constant (K_{obs}) for the duplex formation is given as

$$\frac{d \ln K_{\text{obs}}}{d \ln a_w} = - \left[\Delta n_w + \Delta n_{\text{os}} \left[\frac{d \ln a_{\text{os}}}{d \ln a_w} \right] + \Delta n_{\text{Na}^+} \left[\frac{d \ln a_{\text{Na}^+}}{d \ln a_w} \right] \right] \quad (6)$$

where, a_w , a_{os} , and a_{Na^+} are the activities of water, osmolyte and sodium ion, respectively.

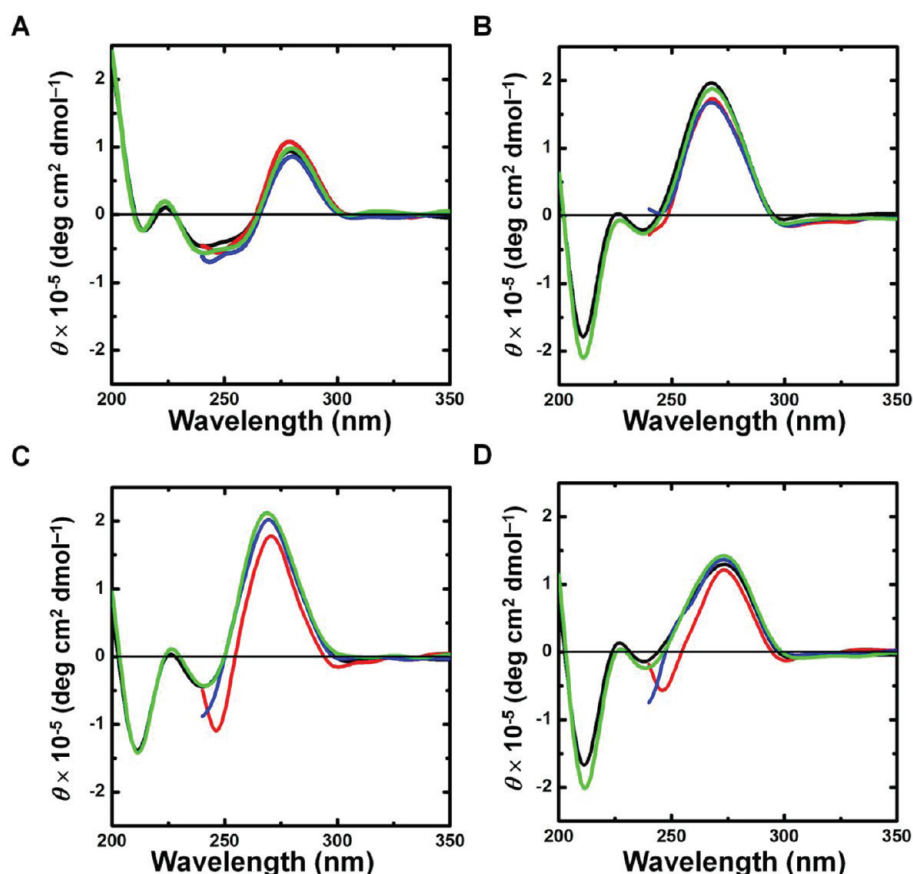


Figure 1. CD spectra of 20 μM (A) DNA duplex, (B) RNA duplex, (C) DNA/RNA hybrid, and (D) RNA/DNA hybrid in 10 mM sodium phosphate (pH 7.0), 1 M NaCl, and 1 mM Na_2EDTA at 4 $^\circ\text{C}$ without any osmolyte (black), 40 wt % PEG 200 (green), 40 wt % proline (blue), and 40 wt % trimethylglycine (red).

MD Simulations. The Discovery Studio Molecular Simulations package with CHARMM force field was used for MD simulations. The DNA duplex was constructed as a B-form helix. The RNA duplex and the DNA/RNA and RNA/DNA hybrids were constructed as A-form helices. An explicit periodic boundary model was employed to simulate solvent molecules (water) around nucleic acid duplexes. A smart minimizer algorithm with 5000 steps was used for the initial energy minimization. The energy minimization, heating, equilibration, and production MD simulations were performed using the Standard Dynamic Cascade protocol. The hydrated nucleic acid duplex systems were then optimized (10 000 steps), heated to a specific target temperature (50 000 steps), equilibrated (500 000 steps), and finally reproduced (200 000 steps). All MD simulations were performed in the NPT ensemble (the number of particles N , the pressure $P = 1$ atm, and the temperature T of the system were kept constant). A sequential step of 1.0 fs was applied for all simulations. The water molecules, including the second layer of the hydration shell, were counted manually in each of the simulated structures. Global flexibilities of the nucleic acid duplex structures were compared by monitoring the root-mean-square displacement (rmsd) of the structures after the MD simulation runs at different target temperatures.

RESULTS

Effects of Molecular Crowding Simulated by Osmolytes on the Hybrid Nucleic Acid Duplexes. The helical conformations of

the DNA/RNA hybrid, RNA/DNA hybrid, DNA duplex, and RNA duplex were investigated using CD measurements both in the absence and in the presence of molecular crowding agents. The CD spectrum of a 20 μM DNA duplex under dilute conditions in the absence of osmolytes in a buffer containing 10 mM sodium phosphate (pH 7.0), 1 M NaCl, and 1 mM Na_2EDTA was typical of a B-form duplex with a positive peak at around 280 nm (Figure 1A), indicating that an intermolecular and antiparallel duplex was formed.^{59–61} The CD spectrum of 20 μM RNA duplex under the same conditions had a positive peak around 270 nm, a weak negative peak around 235 nm, and an intense negative peak at 210 nm (Figure 1B), indicating that the duplex adopted an A-form structure.^{59–61}

In the absence of osmolytes, the CD spectra of DNA/RNA and RNA/DNA hybrids were different from the CD spectra of DNA and RNA duplexes (Figure 1); the CD spectra of the hybrids also differed from each other. The CD spectra of DNA/RNA hybrid in the absence of osmolytes had an intense positive peak around 270 nm, a relatively weak negative peak around 240 nm, and an intense negative peak at 210 nm (Figure 1C). Thus, the structure of the DNA/RNA hybrid appeared to be intermediate between structures of the A- and B-form double helices. The CD spectrum of the RNA/DNA hybrid also appeared to be intermediate between those of the DNA and RNA duplexes with a positive peak positioned around 273 nm, a minor negative peak around 235 nm, and an intense negative peak at 210 nm in the absence of osmolytes (Figure 1D). The intensity of the negative band at 210 nm is reflective of the

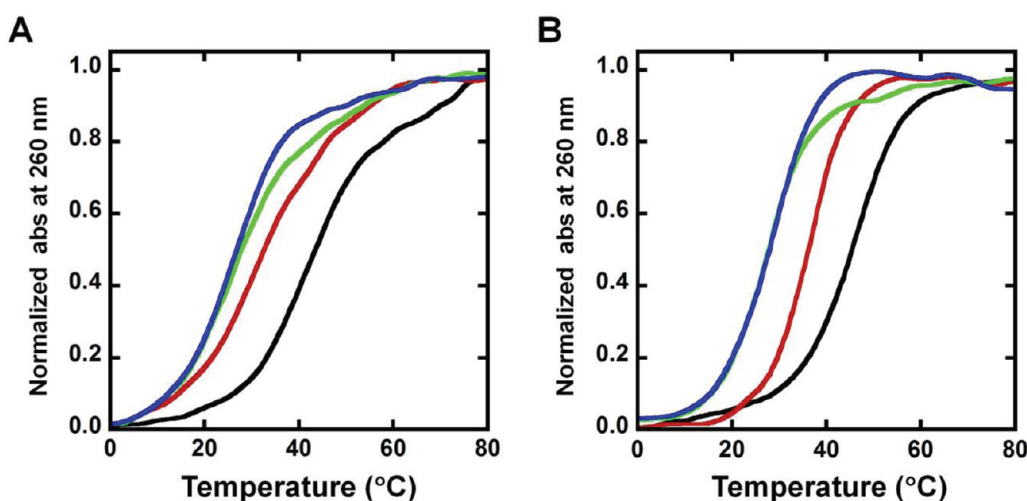


Figure 2. Normalized UV melting curves of (A) 5 μ M DNA/RNA and (B) 5 μ M RNA/DNA hybrids at 260 nm in a buffer containing 10 mM sodium phosphate (pH 7.0), 1 M NaCl, and 1 mM Na₂EDTA without any cosolute (black), in 40 wt % PEG 200 (blue), in 40 wt % proline (green), and in 40 wt % trimethylglycine (red).

Table 1. Thermodynamic Parameters for the Structural Formations of DNA/RNA Hybrid ^a

osmolyte (wt %)	ΔH° (kcal mol ⁻¹)	$T\Delta S^\circ$ (kcal mol ⁻¹)	ΔG_{25}° (kcal mol ⁻¹)	T_m (°C)
none	-60.2 ± 3.9	-49.3 ± 3.5	-10.9 ± 0.1	42.0
10% PEG 200	-54.9 ± 3.3	-45.0 ± 3.1	-9.9 ± 0.1	39.0
20% PEG 200	-51.4 ± 2.5	-42.5 ± 2.6	-8.9 ± 0.1	35.5
30% PEG 200	-48.3 ± 2.6	-40.1 ± 2.3	-8.2 ± 0.1	32.0
40% PEG 200	-43.3 ± 3.9	-35.9 ± 3.7	-7.4 ± 0.1	26.0
10% Proline	-54.9 ± 1.7	-45.1 ± 1.8	-9.8 ± 0.1	38.0
20% Proline	-52.2 ± 2.4	-43.3 ± 2.2	-8.9 ± 0.1	34.5
30% Proline	-48.5 ± 2.8	-40.6 ± 2.4	-7.9 ± 0.1	29.0
40% Proline	-45.0 ± 2.9	-37.9 ± 2.7	-7.1 ± 0.1	24.5
10% Trimethylglycine	-57.1 ± 5.4	-46.8 ± 5.0	-10.3 ± 0.2	40.0
20% Trimethylglycine	-53.9 ± 3.0	-44.0 ± 3.4	-9.9 ± 0.1	39.0
30% Trimethylglycine	-50.4 ± 3.8	-40.9 ± 3.5	-9.5 ± 0.1	36.5
40% Trimethylglycine	-47.3 ± 3.9	-38.5 ± 3.7	-8.8 ± 0.1	33.0

^a All experiments were carried out in a buffer containing 10 mM sodium phosphate (pH 7.0), 1 M NaCl, and 1 mM Na₂EDTA and various concentrations of osmolytes. Values are mean \pm standard deviation from the curve fitting and T_m^{-1} vs $\ln(C_t)$ plots. Melting temperatures were measured at a total strand concentration of 5 μ M.

backbone conformation. The CD signature of the RNA/DNA hybrid resembled the canonical A-form helix. An extensive literature survey revealed that hybrids with purine-rich RNA strands have spectra more like the canonical A-form helix than those with pyrimidine-rich RNA strands.^{38,62–65} Hence, in the absence of osmolytes, our results were consistent with the previous reports.

In the presence of 40 wt % PEG 200, trimethylglycine, or proline, the CD signatures of all four duplexes were unaltered compared to those in the buffer alone, indicating no structural modification by the osmolytes studied here (Figure 1). The CD spectra below 230 nm in the presence of trimethylglycine or proline are not shown because there were changes in that region due to the significant contribution of the osmolytes to the CD spectra. These data indicate that these duplexes can be used to investigate the quantitative effects of the osmolytes on the thermodynamics of A-form, B-form, and the intermediate duplexes.

Thermal Stability of Hybrids in the Presence of Osmolytes. UV melting curves of duplexes, prepared at concentrations from

2 μ M to 200 μ M, were obtained at 260 nm in the absence and presence of the osmolytes in a buffer containing 10 mM sodium phosphate (pH 7.0), 1 M NaCl, and 1 mM Na₂EDTA (Figure 2 and Supporting Information Figures S1 and S2). In the absence of any osmolyte, the order of thermal stabilities of nucleic acid duplexes was DNA/DNA \approx DNA/RNA < RNA/DNA < RNA/RNA. The melting temperatures (T_m 's) of the duplexes decreased gradually as osmolyte concentration was increased from 0 to 40 wt % (Tables 1 and 2, Figure 2, and Supporting Information Figures S1 and S2). Figure 2A shows representative UV melting curves of 5 μ M DNA/RNA hybrid duplex in the presence of 40 wt % of each osmolyte. The T_m was 42.0 °C in the absence of any osmolyte, and T_m 's were 26.0, 24.5, and 33.0 °C in the presence of 40 wt % PEG 200, proline, and trimethylglycine, respectively (Table 1). T_m 's of the transitions of 5 μ M RNA/DNA hybrid were 45.2 °C in the absence of any osmolyte and 27.6, 25.8, and 35.7 °C in the presence of 40 wt % PEG 200, proline, and trimethylglycine, respectively (Figure 2B and Table 2). The RNA/DNA hybrid, which contains the purine-rich RNA strand, melted at higher

Table 2. Thermodynamic Parameters for the Structural Formations of RNA/DNA Hybrid ^a

osmolyte (wt %)	ΔH° (kcal mol ⁻¹)	$T\Delta S^\circ$ (kcal mol ⁻¹)	ΔG°_{25} (kcal mol ⁻¹)	T_m (°C)
none	-66.8 ± 1.3	-54.8 ± 1.2	-12.0 ± 0.1	45.2
10% PEG 200	-60.0 ± 2.5	-48.9 ± 2.1	-11.1 ± 0.2	41.7
20% PEG 200	-54.9 ± 1.9	-44.7 ± 1.6	-10.2 ± 0.3	38.5
30% PEG 200	-51.7 ± 2.3	-42.3 ± 2.0	-9.4 ± 0.4	34.6
40% PEG 200	-44.9 ± 3.0	-36.4 ± 2.5	-8.5 ± 0.3	27.6
10% Proline	-58.3 ± 2.6	-47.2 ± 2.1	-11.1 ± 0.3	40.1
20% Proline	-53.9 ± 2.5	-43.6 ± 2.0	-10.3 ± 0.2	35.1
30% Proline	-51.6 ± 2.9	-42.5 ± 2.4	-9.1 ± 0.5	30.6
40% Proline	-47.8 ± 3.0	-39.7 ± 2.5	-8.1 ± 0.4	25.8
10% Trimethylglycine	-62.9 ± 1.5	-51.4 ± 1.3	-11.5 ± 0.1	42.8
20% Trimethylglycine	-60.8 ± 1.5	-49.7 ± 1.2	-11.1 ± 0.3	40.7
30% Trimethylglycine	-57.4 ± 1.7	-47.0 ± 1.5	-10.4 ± 0.2	38.8
40% Trimethylglycine	-52.7 ± 1.5	-42.8 ± 1.3	-9.8 ± 0.4	35.7

^a All experiments were carried out in a buffer containing 10 mM sodium phosphate (pH 7.0), 1 M NaCl, 1 mM Na₂EDTA, and various concentrations of osmolytes. Values are mean ± standard deviation from the curve fitting and T_m^{-1} vs $\ln(C_t)$ plots. Melting temperatures were measured at a total strand concentration of 5 μ M.

temperatures under all conditions than did the DNA/RNA hybrid. Under these dilute conditions, the difference in thermal stability of hybrids was consistent with previous results.^{36,66,67} UV melting curves of the DNA duplex and the RNA duplex were also acquired at 260 nm with and without osmolytes. The T_m 's of these duplexes decreased gradually with increasing concentrations of PEG 200, proline, and trimethylglycine (Supporting Information Figures S3 and S4, Table S1 and Table S2). The trends of destabilization of the DNA and RNA duplexes were similar to those of the hybrids; the effect of proline was similar to that of PEG 200, and trimethylglycine was not as destabilizing.

Effect of Osmolytes on the Thermodynamic Parameters of Nucleic Acid Structure Formation. From the UV melting curves, we calculated thermodynamic parameters as described in the Materials and Methods section (eqs 1 and 2). The values of ΔH° , $T\Delta S^\circ$, and ΔG° at 25 °C (ΔG°_{25}) for all the duplexes studied here are shown in Tables 1 and 2. Using the free energies of stabilization for all nearest-neighbor base pair sets,^{32,33,68} values of ΔG° at 37 °C (ΔG°_{37}) were estimated as -9.0, -8.6, -8.3, and -12.6 kcal mol⁻¹ for the DNA/DNA, DNA/RNA hybrid, RNA/DNA hybrid, and RNA/RNA duplexes, respectively. The ΔG°_{37} values calculated from melting curves were -8.9, -8.9, -9.7, and -12.9 kcal mol⁻¹ for the DNA/DNA, DNA/RNA hybrid, RNA/DNA hybrid, and RNA/RNA duplexes, respectively. Thus, predictions utilizing the nearest neighbor model are in good agreement with the free energies obtained from the melting curves with the exception of that for the RNA/DNA hybrid. The discrepancy between the calculated and the measured ΔG°_{37} for the RNA/DNA hybrid is likely due to the fact that the nearest neighbor model data that we used to calculate the ΔG°_{37} were obtained by averaging the melting data over a large number of sequences. Such disagreement between the calculated and the measured values for nucleic acids hybrid were reported previously.⁶⁹ In the absence of any osmolyte, the order of the ΔG°_{25} for the formation of nucleic acid duplexes was DNA/DNA \approx DNA/RNA < RNA/DNA < RNA/RNA. The difference in the stabilities of hybrids of mixed base sequence context has been observed previously in optical melting experiments, and the hybrids with purine-rich RNA strands are more stable than those with pyrimidine-rich RNA strands.^{36,66,67} Moreover, the dA-rU

base pair destabilizes the neighboring dG-rC base pair.⁶⁹ Thus, ΔG°_{25} values for the formation of hybrids studied here are in agreement with previous studies.^{32,36}

In the presence of 40 wt % PEG 200, the values of ΔH° and $T\Delta S^\circ$ for formation of the DNA/RNA hybrid increased from -60.2 to -43.3 kcal mol⁻¹ and -49.3 to -35.9 kcal mol⁻¹, respectively (Table 1). Consequently, the ΔG°_{25} for formation of the hybrid increased from -10.9 to -7.4 kcal mol⁻¹. This indicated that destabilization of the hybrid duplex was due to an unfavorable enthalpic contribution in the presence of PEG 200. As in the presence of PEG, there was an increase in the values of ΔH° (-60.2 to -45.0 kcal mol⁻¹), $T\Delta S^\circ$ (-49.3 to -37.9 kcal mol⁻¹), and ΔG°_{25} (-10.9 to -7.1 kcal mol⁻¹) for the formation of the DNA/RNA hybrid in 40 wt % proline compared to buffer alone. Trimethylglycine also had an unfavorable enthalpic effect on the thermodynamic stability of the hybrid (Table 1). In the presence of PEG 200, proline, or trimethylglycine, the RNA/DNA hybrid formation (Table 2) and DNA and RNA duplex formation were also enthalpy driven (Supporting Information Table S1 and S2) as reported previously by our group.¹⁷⁻¹⁹ In the absence of the osmolytes, the ΔG°_{25} value of the DNA/RNA hybrid was -10.9 kcal mol⁻¹, which was nearly identical to that of the DNA duplex (-10.6 kcal mol⁻¹). The ΔG°_{25} value of the RNA/DNA hybrid duplex was -12.0 kcal mol⁻¹, intermediate between that of DNA duplex (-10.6 kcal mol⁻¹) and that of the RNA duplex (-15.5 kcal mol⁻¹). In the presence of 40 wt % osmolyte, ΔG°_{25} values of both hybrids were closer to that of the DNA duplex than the RNA duplex.

To compare the effect of each osmolyte on the duplex stabilities, we evaluated the $\Delta\Delta G^\circ_{25}$, the difference between the ΔG°_{25} of nucleic acid structures in the presence of the osmolyte and that in the absence of the osmolyte. For example, in the presence of 40 wt % PEG 200, the $\Delta\Delta G^\circ_{25}$ values were +3.0, +3.5, +3.5, and +4.1 kcal mol⁻¹ for the DNA/DNA, DNA/RNA hybrid, RNA/DNA hybrid, and RNA/RNA, respectively. The $\Delta\Delta G^\circ_{25}$ values in the presence of 40 wt % proline were estimated to be +3.5, +3.8, +3.9, and +4.8 kcal mol⁻¹, and those in trimethylglycine were +1.5, +2.1, +2.2, and +2.7 kcal mol⁻¹ for the DNA/DNA, DNA/RNA hybrid, RNA/DNA hybrid, and RNA/RNA, respectively. For each osmolyte, it is noteworthy that the

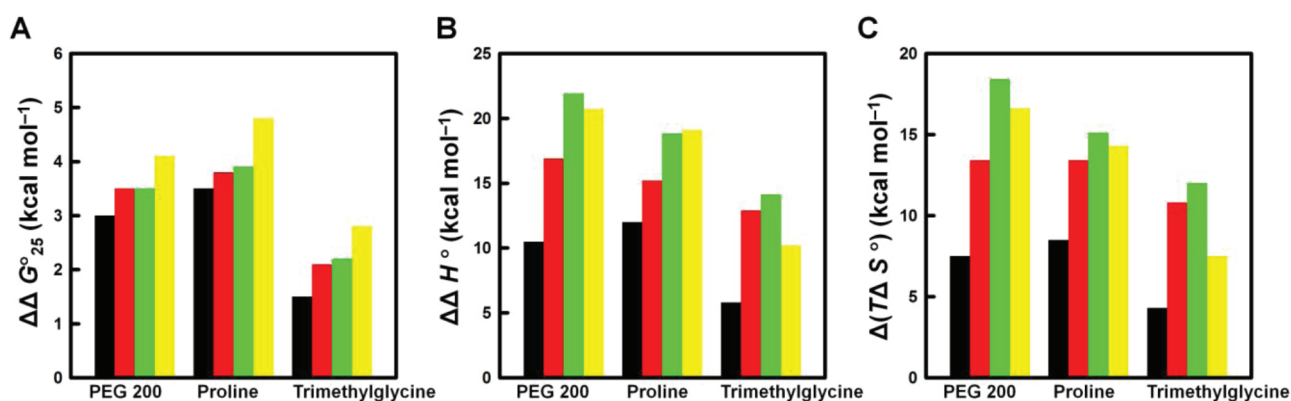


Figure 3. (A) $\Delta\Delta G_{25}^{\circ}$, (B) $\Delta\Delta H^{\circ}$, and (C) $\Delta(T\Delta S^{\circ})$ in the presence of PEG 200, proline, and trimethylglycine for DNA duplex (black), DNA/RNA hybrid (red), RNA/DNA hybrid (green), and RNA duplex (yellow).

$\Delta\Delta G_{25}^{\circ}$ values for the formation of both hybrids were intermediate between those of the RNA duplex and the DNA duplex (Figure 3A). We then evaluated $\Delta\Delta H^{\circ}$ ($= (\Delta H^{\circ}$ of nucleic acid structures in the presence of the osmolyte) $- (\Delta H^{\circ}$ of nucleic acid structures in the absence of the osmolyte)) and $\Delta(T\Delta S^{\circ})$ ($= (T\Delta S^{\circ}$ of nucleic acid structures in the presence of the osmolyte) $- (T\Delta S^{\circ}$ of nucleic acid structures in the absence of the osmolyte)) at 25 °C. Surprisingly, for 40 wt % PEG 200 and proline, the $\Delta\Delta H^{\circ}$ and $\Delta(T\Delta S^{\circ})$ values for the RNA/DNA hybrid formation were closer to those of RNA duplex than those of DNA duplex (Figures 3B and 3C). The DNA/RNA hybrid values were intermediate between those of the RNA duplex and the DNA duplex in the presence of 40 wt % PEG 200 and proline (Figures 3B and 3C). Trimethylglycine was the exception, probably due to the weak and noncooperative interaction of trimethylglycine with AT base pairs in the major groove (Figures 3B and 3C).⁷⁰ Interestingly, the plot of ΔH° versus ΔS° for all duplexes revealed a good linear correlation (Figure 4). For the formation of hybrids, the high enthalpic exothermicities were compensated by entropic contributions, resulting in comparatively small ΔG_{25}° values. Owing to the enthalpy–entropy compensation phenomenon, the net free energy of folding ($\Delta\Delta G_{25}^{\circ}$) of hybrids were intermediate between those of DNA duplex and RNA duplex and the order of net stabilities of the hybrids was different from that of the net change in enthalpic exothermicities ($\Delta\Delta H^{\circ}$) and rotational penalties ($\Delta(T\Delta S^{\circ})$).

Hydration Change upon Hybrid Formation. To further examine the effect of the osmolytes on the thermodynamic stability of the hybrids, we used a previously reported method^{17–19} to investigate how water molecules affect the thermodynamics of the hybrids. The thermodynamic behaviors observed with PEG 200, proline, and trimethylglycine were similar to those in the previous reports of the effects of molecular crowding on the thermodynamics of the DNA duplex formation, suggesting that hydration is an important factor in stability.^{17–19} Figure 5 shows the plots of $\ln K_{\text{obs}}$ (the observed equilibrium constant) versus $\ln a_w$ (the water activity) determined by osmotic pressure measurements (Materials and Methods section, eqs 3 and 4) at 25 °C for the formation of the hybrids in the presence of the osmolytes (Supporting Information Table S3). The plots reveal that $\ln K_{\text{obs}}$ in the presence of each osmolyte increased linearly with increasing $\ln a_w$ (Figure 5). The linearity of the plots suggests that the slope of these plots is approximately equal to the constant term $-\Delta n_w$, which is the number of water molecules bound upon formation of a structure

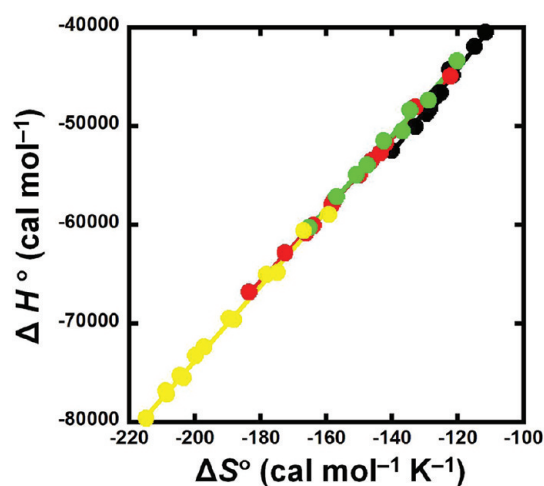


Figure 4. Enthalpy–entropy compensation plot for the folding thermodynamics of DNA duplex (black), DNA/RNA hybrid (green), RNA/DNA hybrid (red), and RNA duplex (yellow).

(Materials and Methods section, eq 6).^{17–19} From the slopes of the plots, we estimate that upon formation of the DNA/RNA hybrid, 96.9, 84.2, and 42.5 waters per duplex structure were taken up in the presence of PEG 200, proline, and trimethylglycine, respectively (Figure 6). The RNA/DNA hybrid duplex structure took up 96.8, 86.8, and 47.7 waters per duplex structure in the presence of PEG 200, proline, and trimethylglycine, respectively (Figure 6). The numbers of water molecules taken up as the DNA duplex structure formed in the presence of PEG 200, proline, and trimethylglycine were estimated to be 83.3, 77.7, and 32.5 per duplex structure, respectively (Figure 6 and Supporting Information Figure S5). The numbers of water molecules per RNA duplex structure were higher at 114, 109, and 57.1 waters per duplex in the presence of PEG 200, proline, and trimethylglycine, respectively (Figure 6 and Supporting Information Figure S5). These results demonstrated that hydration for each hybrid was almost identical in the presence of PEG 200 and proline but was lower in the presence of trimethylglycine. The lesser extent of hydration in the presence of trimethylglycine is possibly due to the interaction of trimethylglycine with AT base pairs in the major groove, which may lead to release of water molecules from these sites.⁷⁰ Roughly half the numbers of waters were bound per duplex in the presence of trimethylglycine as in the other osmolytes.

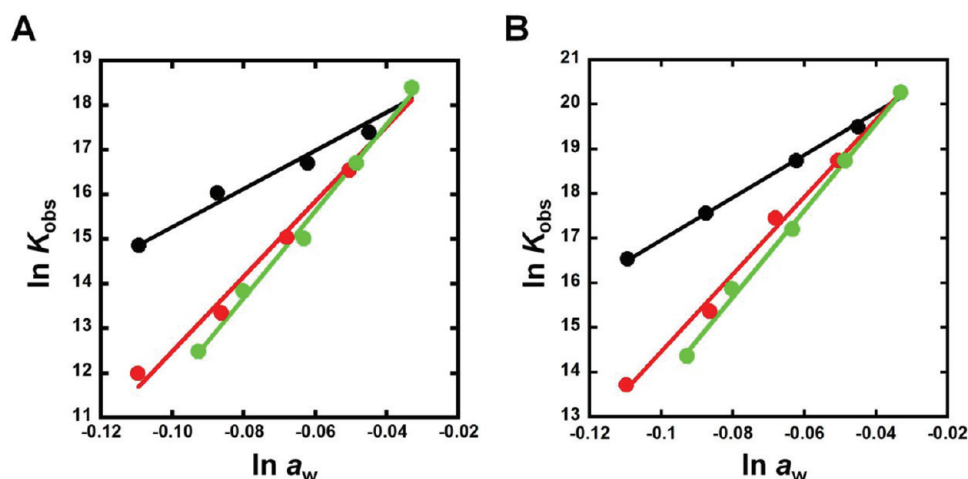


Figure 5. Plots of $\ln K_{\text{obs}}$ versus $\ln a_w$ for (A) DNA/RNA hybrid and (B) RNA/DNA hybrid in the presence of PEG 200 (green), proline (red), and trimethylglycine (black) in a buffer containing 10 mM sodium phosphate (pH 7.0), 1 M NaCl, and 1 mM Na_2EDTA with 0, 10, 20, 30, and 40 wt % osmolytes at 25 °C.

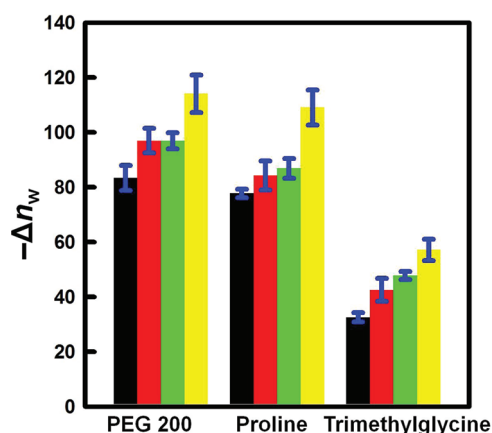


Figure 6. The $-\Delta n_w$ values at 25 °C for DNA duplex (black), DNA/RNA hybrid (red), RNA/DNA hybrid (green), and RNA duplex (yellow) in the presence of PEG 200, proline, and trimethylglycine.

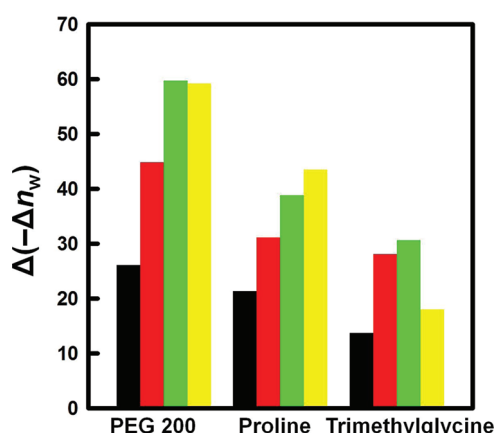


Figure 7. Changes in $-\Delta n_w$ values for DNA duplex (black), DNA/RNA hybrid (red), RNA/DNA hybrid (green), and RNA duplex (yellow) in the presence of PEG 200, proline, and trimethylglycine.

This is reasonable since the sequence studied here has $\sim 40\%$ AT base pairs. The $-\Delta n_w$ values of both hybrids were intermediate between those of DNA and RNA duplexes. The 2' hydroxyls in the ribose sugars of RNA strands strongly interact with water in an RNA duplex.⁷¹ Therefore, the DNA/RNA and RNA/DNA hybrids were more highly hydrated than the DNA duplex at 25 °C due to the hydration of 2' hydroxyls in the RNA strand.

It is important to note that differences in ΔG°_{25} and hydration at 25 °C of the DNA/RNA and RNA/DNA hybrids in the presence and absence of osmolyte were identical and intermediate between those of RNA duplex and DNA duplex. In contrast, $\Delta\Delta H^\circ$ and $\Delta(T\Delta S^\circ)$ at 25 °C of the DNA/RNA hybrid were intermediate between those of DNA duplex and RNA duplex, whereas $\Delta\Delta H^\circ$ and $\Delta(T\Delta S^\circ)$ at 25 °C of the RNA/DNA hybrid were closer to values for the RNA duplex than those of the DNA duplex. Therefore, $\Delta\Delta H^\circ$ and $\Delta(T\Delta S^\circ)$ of the hybrids were affected by factors other than hydration.

Temperature-Dependent Changes in Hydration upon the Hybrid Formation. To characterize hybrid duplex hydration further, we estimated the hydration of each duplex in the presence of osmolytes at 0 and 37 °C (Supporting Information

Figure S6). In the absence of osmolyte, the hydration of DNA/RNA hybrid was intermediate between RNA and DNA duplexes at both temperatures, whereas the hydration of RNA/DNA hybrid was, interestingly, closer to that of the RNA duplex at 0 °C and closer to that of the DNA duplex at 37 °C. To compare the effect of temperature on the hydration of different hybrid formations, we evaluated the change of hydration ($\Delta(-\Delta n_w) = (-\Delta n_w \text{ at } 0^\circ\text{C}) - (-\Delta n_w \text{ at } 37^\circ\text{C})$) of nucleic acid structures with temperature (Figure 7). In the presence of PEG 200, the $\Delta(-\Delta n_w)$ s were 26.1, 44.8, 59.7, and 59.2 per duplex structure for the DNA/DNA, DNA/RNA hybrid, RNA/DNA hybrid, and RNA/RNA, respectively. In the presence of proline, the values were estimated to be 21.3, 31.1, 38.8, and 43.5 per duplex structure for the DNA/DNA, DNA/RNA hybrid, RNA/DNA hybrid, and RNA/RNA, respectively. The $\Delta(-\Delta n_w)$ s were significantly lower in the presence of trimethylglycine: 13.7, 28.1, 30.6, and 18.0 per duplex structure for the DNA/DNA, DNA/RNA hybrid, RNA/DNA hybrid, and RNA/RNA, respectively. In the presence of all three osmolytes tested here, the $\Delta(-\Delta n_w)$ value for the RNA/DNA hybrid formation was higher than that for DNA/RNA hybrid formation (Figure 7). This

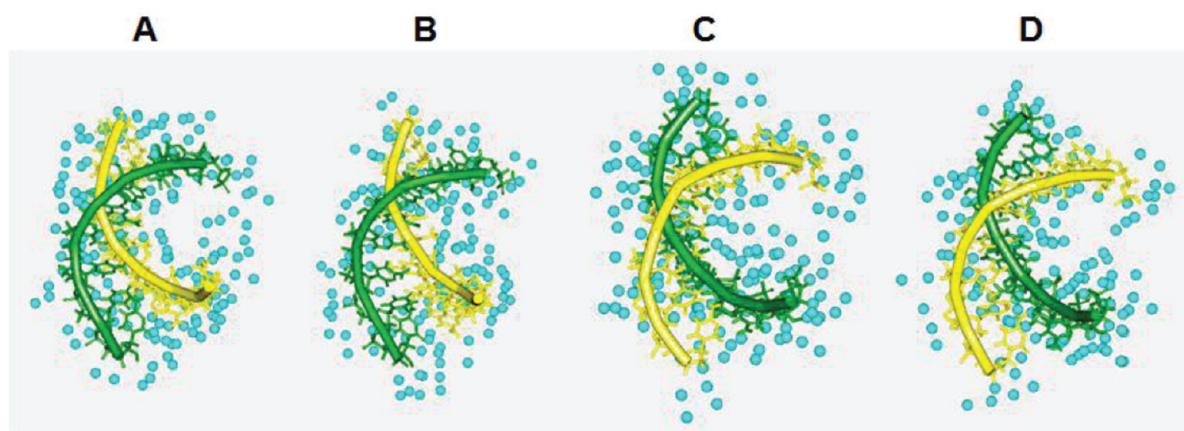


Figure 8. Snapshots of MD simulations for (A) the DNA/RNA hybrid at 0 °C, (B) the DNA/RNA hybrid at 37 °C, (C) the RNA/DNA hybrid at 0 °C, and (D) the RNA/DNA hybrid at 37 °C. DNA strand (yellow), RNA strand (green), and water (cyan).

Table 3. Number of Water Molecules Bounds Per Duplex Structure^a

temperature (°C)	DNA/DNA	DNA/RNA	RNA/DNA	RNA/RNA
0	128 ± 2	163 ± 2	182 ± 1	189 ± 3
37	119 ± 2	152 ± 1	159 ± 2	169 ± 3

^a Values are mean ± standard deviation of at least three snapshots. The water molecules, including the second layer of the hydration shell, in the simulated structures were manually counted.

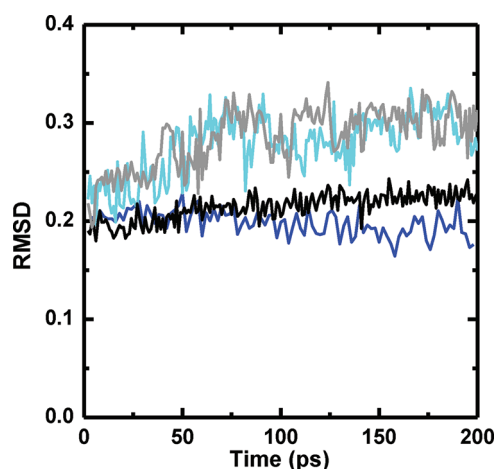


Figure 9. Time evolution of rmsd in MD simulations for the DNA/RNA hybrid at 0 °C (black line) and 37 °C (gray line) and the RNA/DNA hybrid at 0 °C (blue line) and 37 °C (cyan line).

suggests that temperature-dependent structural properties of hybrid duplexes, which are accompanied by changes in hydration, differ between RNA/DNA and DNA/RNA hybrids and that these differences result from the differences in $\Delta\Delta H^\circ$ and $\Delta(T\Delta S^\circ)$.

MD Simulation of the Hybrids. We carried out MD simulations of the hydrated nucleic acid structures at 0 and 37 °C (Figure 8 and Figure S7) to estimate the number of water molecules bound to the final duplex structures (Table 3). The water molecules, including those in the second layer of the hydration shell, were counted manually in each simulated structure.

The change in the number of water molecules bound to the RNA/DNA hybrid at 0 °C compared to 37 °C was larger than that of the DNA/RNA hybrid. Additionally, we compared global flexibilities of the nucleic acid structures by monitoring the rmsd values of the global duplex structures during the MD simulation runs at 0 and 37 °C (Figure 9 and Supporting Information Figure S8). The difference of rmsd values between 0 and 37 °C for the RNA/DNA hybrid was larger than that for the DNA/RNA hybrid, suggesting that the RNA/DNA hybrid was more flexible than the DNA/RNA hybrid (Figure 9). These MD simulations suggest that the larger change in hydration of the RNA/DNA hybrid compared to the DNA/RNA hybrid was mainly due to differences in hydration of the major groove. We hypothesize that the higher flexibility of the RNA/DNA hybrid compared to the DNA/RNA hybrid is due to loss of major groove hydration at higher temperature.

DISCUSSION

Hybrids formed by one RNA strand and one DNA strand have unique structures. Early fiber diffraction and X-ray data suggested that hybrid structures were similar to the canonical A-form helix,²² and X-ray crystallographic data showed that all ribose sugars and the majority of the 2'-deoxyriboses adopted the north conformation, characteristic of an RNA duplex.^{24,29} In solution, however, NMR, CD, and Raman spectroscopy revealed that a considerable portion of 2'-deoxyriboses in hybrids exist in the south conformation, typical of B-DNA.^{23,25} Recent NMR studies reached the same conclusion: The structure of a hybrid is an intermediate between A-form and B-form helices.^{27,28,30} An NMR study by Gyi et al. indicated that the deoxyriboses in a hybrid are more flexible than those in a DNA duplex.⁷² Recent MD simulations revealed that the structural parameters of the hybrid are closer to those of an RNA duplex, but the hybrid is closer to the DNA duplex in terms of structural disorder.⁷³ There were no clear differences among the global flexibilities of the hybrid, DNA duplex, and RNA duplex, however, in these simulations. Another recent report on the structure and dynamics of a hybrid suggests that flexibility is decreased compared with that of an RNA duplex and that the minor groove width of the hybrid is narrower than that in the RNA duplex.⁷⁴ These results demonstrate that the structures and flexibilities of hybrid are sensitive to both solvent conditions and the base sequences.

In the present study, CD spectra showed that the structures of the DNA/RNA and the RNA/DNA hybrids were intermediate between those of A- and B-form helices. For the sequence studied here, the spectrum of the RNA/DNA hybrid, which contains the purine-rich RNA strand, was closer to that of the canonical A-form helix than the spectrum of the DNA/RNA hybrid. In addition, in the presence of all three osmolytes tested in this study, the $\Delta(-\Delta n_w)$ value for the RNA/DNA hybrid formation was higher than that of DNA/RNA hybrid formation (Figure 7). We estimated the number of water molecules bound to the final duplex structures by evaluation of the slope of the $\ln K_{\text{obs}}$ versus $\ln a_w$ plot obtained using osmotic pressure measurements; the experiments thus determined differences in the number of water molecules bound to single-strands and the duplexes rather than the total number of waters bound. In MD simulations, the change in the number of water molecules bound to the RNA/DNA hybrid at 0 °C compared to 37 °C was also larger than that of the DNA/RNA hybrid. Even though the hydration condition of the single-stranded state is not known, the hydration states of the hybrid structures estimated from the MD simulations at different temperatures are correlated with experimental data. Furthermore, the difference of rmsd values between 0 and 37 °C for the RNA/DNA hybrid was larger than for the DNA/RNA hybrid, suggesting that the RNA/DNA hybrid was more flexible than the DNA/RNA hybrid (Figure 9). Thus, sequence-specific hydration changes in hybrids are probably due to the differences in flexibility.

Together with hydrogen bonding and base stacking interactions between base pairs determined by sequence and the backbone chemistry, solution conditions play an important role in the thermodynamic stabilities of duplex formation. The osmotic environment influences the number of water molecules associated with a nucleic acid structure and thus could determine the stability or conformation of the helix. Cosolutes such as PEG 200 act to reduce the water activity of a solution and thereby influence the thermodynamic stability of nucleic acids.^{17–19} Additionally, the reduced water activity can lead to conformational polymorphism and stabilize noncanonical DNA structures^{75–77} even though, the high molecular weight crowding agents have no effect on the same noncanonical DNA structures.⁷⁸ Moreover, counterion condensation is reduced in the presence of PEG.^{20,79} Osmolytes also have an excluded volume effect that has been studied extensively for proteins.^{3,80,81} Recently, stabilization of folded RNA structure through the excluded volume effect of PEG 1000 was reported.⁸² Spink and Chaires clearly showed effects of osmolytes on the behavior of DNA,⁸³ and a MD simulation suggested that size and shape of the osmolyte affected the mechanism and degree of the crowding effect.⁸⁴ For each osmolyte evaluated here, the $\Delta\Delta H^\circ$ values for hybrids determined by comparing duplex formation with and without osmolyte were intermediate between those of RNA and DNA duplex or closer to that of RNA duplex. Therefore, the presence of osmolytes had an unfavorable enthalpic effect on the hydration and helical structure in thermodynamic stabilities of the hybrids studied here. This indicates that it is important to consider the helical conformation of duplexes during the design of nucleic acids drugs.

It has been reported that the flexibility of a hybrid plays a biologically an important role in recognition by enzymes. Conformational flexibility^{73,85–87} and hydration pattern⁸⁸ impact RNase H efficiency. Furthermore, the flexibility of the hybrids influences recognition by the reverse transcriptases of HIV-1 and the *Saccharomyces cerevisiae* LTR-retrotransposon Ty3^{89–91} and by the RNA-induced silencing complex.⁹² Therefore, the

flexibility and hydration of hybrids is relevant to the design of oligonucleotide therapies and to elucidation of the biological mechanisms of reverse transcriptases and RNA silencing. Moreover, there are also some intriguing reports about the biological evolution for the structural dynamics of nucleic acids: Genomic structures of microorganisms adapted to high growing temperatures are more rigid than that at low growing temperature.⁹³ In vitro selection of DNA duplexes in the presence of a transcription factor demonstrates that temperature and salt concentration alter the base-sequence selectivity of binding, indicating that the conformational properties of duplex structures are affected by the environment.⁹⁴ Our study suggests that molecular crowding agents are biophysical tools that can be used to shed light on structure and hydration state of nucleic acids.

CONCLUSIONS

In conclusion, our experimental findings revealed that helix stability depends on the osmotic pressure induced by the low molecular weight osmolytes. The degrees of destabilization of nucleic acid duplexes depended on the nucleic acid type: The destabilization of hybrids was intermediate between that of DNA and RNA duplexes at 25 °C. In the presence of low molecular weight osmolytes, destabilization of nucleic acid hybrids primarily originated from differential hydration. The change in the numbers of water molecules bound at 0 and at 37 °C for the RNA/DNA hybrid was higher than that of the DNA/RNA hybrid. This difference was due to the higher $\Delta\Delta H^\circ$ and $\Delta\Delta S^\circ$ values of the RNA/DNA hybrid, which was suggested consequently the global flexibility of RNA/DNA hybrid structure is higher than that of DNA/RNA hybrid by MD simulations. Accordingly, higher unfavorable enthalpy changes ($\Delta\Delta H^\circ$) for the hybrids in the presence of osmolytes are probably the consequence of conformation and hydration. Thus, under molecular crowding conditions with low molecular weight osmolytes, hydration determines the stability and conformation of the helical structure.

ASSOCIATED CONTENT

S Supporting Information. Tables for thermodynamic parameters, UV melting curves, hydration of nucleic acid structures, and molecular dynamics simulations for the nucleic acid structures. This material is available free of charge via the Internet at <http://pubs.acs.org>.

AUTHOR INFORMATION

Corresponding Author

*Fax: +81-78-303-1495. Tel: +81-78-303-1457. E-mail: sugimoto@konan-u.ac.jp.

ACKNOWLEDGMENT

This work was supported in part by Grants in-Aid for Scientific Research, the “Core research” project (2009-2014) from the Ministry of Education, Culture, Sports, Science and Technology, Japan, and the Hirao Taro Foundation of the Konan University Association for Academic Research.

REFERENCES

- (1) Miyoshi, D.; Sugimoto, N. *Biochimie* **2008**, *90*, 1040.
- (2) Nakano, S.; Karimata, H. T.; Kitagawa, Y.; Sugimoto, N. *J. Am. Chem. Soc.* **2009**, *131*, 16881.

- (3) Zimmerman, S. B.; Minton, A. P. *Annu. Rev. Biophys. Biomol. Struct.* **1993**, *22*, 27.
- (4) Yancey, P. H. *J. Exp. Biol.* **2005**, *208*, 2819.
- (5) Gilles, R. *Comp. Biochem. Physiol. A Physiol.* **1997**, *117*, 279.
- (6) Measures, J. C. *Nature* **1975**, *257*, 398.
- (7) Le Rudulier, D.; Strom, A. R.; Dandekar, A. M.; Smith, L. T.; Valentine, R. C. *Science* **1984**, *224*, 1064.
- (8) Perroud, B.; Le Rudulier, D. *J. Bacteriol.* **1985**, *161*, 393.
- (9) Craig, S. A. *Am. J. Clin. Nutr.* **2004**, *80*, 539.
- (10) Holtmann, G.; Bremer, E. *J. Bacteriol.* **2004**, *186*, 1683.
- (11) Bohnert, H. J.; Jensen, R. G. *Trends Biotechnol.* **1996**, *14*, 89–97.
- (12) Rajendrakumar, C. S.; Suryanarayana, T.; Reddy, A. R. *FEBS Lett.* **1997**, *410*, 201.
- (13) Del Vecchio, P.; Esposito, D.; Ricchi, L.; Barone, G. *Int. J. Biol. Macromol.* **1999**, *24*, 361.
- (14) Spink, C. H.; Garbett, N.; Chaires, J. B. *Biophys. Chem.* **2007**, *126*, 176.
- (15) Vasudevamurthy, M. K.; Lever, M.; George, P. M.; Morison, K. R. *Biopolymers* **2009**, *91*, 85.
- (16) Koumoto, K.; Ochiai, H.; Sugimoto, N. *Tetrahedron* **2008**, *64*, 168.
- (17) Nakano, S.; Karimata, H.; Ohmichi, T.; Kawakami, J.; Sugimoto, N. *J. Am. Chem. Soc.* **2004**, *126*, 14330.
- (18) Miyoshi, D.; Karimata, H.; Sugimoto, N. *J. Am. Chem. Soc.* **2006**, *128*, 7957.
- (19) Miyoshi, D.; Nakamura, K.; Tateishi-Karimata, H.; Ohmichi, T.; Sugimoto, N. *J. Am. Chem. Soc.* **2009**, *131*, 3522.
- (20) Karimata, H.; Nakano, S.; Sugimoto, N. *Bull. Chem. Soc. Jpn.* **2007**, *80*, 1987.
- (21) Saenger, W. *Principles of Nucleic Acid Structure*; Springer-Verlag: New York, 1984.
- (22) Milman, G.; Langridge, R.; Chamberlin, M. J. *Proc. Natl. Acad. Sci. U.S.A.* **1967**, *57*, 1804.
- (23) Chou, S. H.; Flynn, P.; Reid, B. *Biochemistry* **1989**, *28*, 2422.
- (24) Katahira, M.; Lee, S. J.; Kobayashi, Y.; Sugeta, H.; Kyogoku, Y.; Iwai, S.; Ohtsuka, E.; Benevides, J. M.; Thomas, G. J., Jr. *J. Am. Chem. Soc.* **1990**, *112*, 4508.
- (25) Hall, K. B.; McLaughlin, L. W. *Biochemistry* **1991**, *30*, 10606.
- (26) Fedoroff, O.; Salazar, M.; Reid, B. R. *J. Mol. Biol.* **1993**, *233*, 509.
- (27) Gonzalez, C.; Stec, W.; Kobylanska, A.; Hogrefe, R. I.; Reynolds, M.; James, T. L. *Biochemistry* **1994**, *33*, 11062.
- (28) Gonzalez, C.; Stec, W.; Reynolds, M. A.; James, T. L. *Biochemistry* **1995**, *34*, 4969.
- (29) Xiong, Y.; Sundaralingam, M. *Nucleic Acids Res.* **2000**, *28*, 2171.
- (30) Gyi, J. I.; Gao, D.; Conn, G. L.; Trent, J. O.; Brown, T.; Lane, A. N. *Nucleic Acids Res.* **2003**, *31*, 2683.
- (31) Sugimoto, N.; Katoh, M.; Nakano, S.; Ohmichi, T.; Sasaki, M. *FEBS Lett.* **1994**, *354*, 74.
- (32) Sugimoto, N.; Nakano, S.; Katoh, M.; Matsumura, A.; Nakamura, H.; Ohmichi, T.; Yoneyama, M.; Sasaki, M. *Biochemistry* **1995**, *34*, 11211.
- (33) Sugimoto, N.; Nakano, S.; Yoneyama, M.; Honda, K. *Nucleic Acids Res.* **1996**, *24*, 4501.
- (34) Sugimoto, N.; Nakano, M.; Nakano, S. *Biochemistry* **2000**, *39*, 11270.
- (35) Wu, P.; Nakano, S.; Sugimoto, N. *Eur. J. Biochem.* **2002**, *269*, 2821.
- (36) Nakano, S.; Kanzaki, T.; Sugimoto, N. *J. Am. Chem. Soc.* **2004**, *126*, 1088.
- (37) Smith, C. A.; Wood, E. J. *Biological Molecules*; 1st ed.; Chapman and Hall: London, 1992.
- (38) Shaw, N. N.; Arya, D. P. *Biochimie* **2008**, *90*, 1026.
- (39) Ogawa, T.; Okazaki, T. *Annu. Rev. Biochem.* **1980**, *49*, 421.
- (40) Varmus, H. E. *Science* **1982**, *216*, 812.
- (41) Al-Hashimi, H. M.; Walter, N. G. *Curr. Opin. Struct. Biol.* **2008**, *18*, 321.
- (42) Rohs, R.; West, S. M.; Sosinsky, A.; Liu, P.; Mann, R. S.; Honig, B. *Nature* **2009**, *461*, 1248.
- (43) Boehr, D. D.; Nussinov, R.; Wright, P. E. *Nat. Chem. Biol.* **2009**, *5*, 789.
- (44) Bothe, J. R.; Lowenhaupt, K.; Al-Hashimi, H. M. *J. Am. Chem. Soc.* **2011**, *133*, 2016.
- (45) Nikolova, E. N.; Kim, E.; Wise, A. A.; O'Brien, P. J.; Andricioaei, I.; Al-Hashimi, H. M. *Nature* **2011**, *470*, 498.
- (46) Kalodimos, C. G.; Biris, N.; Bonvin, A. M.; Levandoski, M. M.; Guennuegues, M.; Boelens, R.; Kaptein, R. *Science* **2004**, *305*, 386.
- (47) Koudelka, G. B.; Mauro, S. A.; Ciubotaru, M. *Prog. Nucleic Acid Res. Mol. Biol.* **2006**, *81*, 143.
- (48) Joshi, R.; Passner, J. M.; Rohs, R.; Jain, R.; Sosinsky, A.; Crickmore, M. A.; Jacob, V.; Aggarwal, A. K.; Honig, B.; Mann, R. S. *Cell* **2007**, *131*, 530.
- (49) Kitayner, M.; Rozenberg, H.; Rohs, R.; Suad, O.; Rabinovich, D.; Honig, B.; Shakked, Z. *Nat. Struct. Mol. Biol.* **2010**, *17*, 423.
- (50) Saiz, L.; Vilar, J. M. *Curr. Opin. Struct. Biol.* **2006**, *16*, 344.
- (51) Khesbak, H.; Savchuk, O.; Tsushima, S.; Fahmy, K. *J. Am. Chem. Soc.* **2011**, *133*, 5834.
- (52) Furse, K. E.; Corcelli, S. A. *J. Phys. Chem. B* **2010**, *114*, 9934.
- (53) Yonetani, Y.; Kono, H. *Biophys. J.* **2009**, *97*, 1138.
- (54) Berg, M. A.; Coleman, R. S.; Murphy, C. J. *Phys. Chem. Chem. Phys.* **2008**, *10*, 1229.
- (55) Yu, H. Q.; Zhang, D. H.; Gu, X. B.; Miyoshi, D.; Sugimoto, N. *Angew. Chem., Int. Ed.* **2008**, *47*, 9034.
- (56) Fasman, G. D. In *Handbook of Biochemistry and Molecular Biology*, 3rd ed.; Richards, E. G., Ed.; CRC Press: Cleveland, OH, 1975; Vol. 1.
- (57) In *Handbook of Biochemistry and Molecular Biology*, 3rd ed.; Richards, E. G., Ed.; CRC Press: Cleveland, OH, 1975; Vol. 1.
- (58) Goobes, R.; Kahana, N.; Cohen, O.; Minsky, A. *Biochemistry* **2003**, *42*, 2431.
- (59) Berova, N.; Nakanishi, K.; Woody, R. W. *Circular Dichroism: Principles and Applications*; 2nd ed.; Wiley-VCH: New York, 2000.
- (60) Bloomfield, V. A.; Crothers, D. M.; Tinoco, Jr. *Nucleic Acids Structures, Properties, and Functions*; University Science Books: Sausalito, CA, 2000.
- (61) Kyrp, J.; Kejniovská, I.; Renciuik, D.; Vorlickova, M. *Nucleic Acids Res.* **2009**, *37*, 1713.
- (62) Ratmeyer, L.; Vinayak, R.; Zhong, Y. Y.; Zon, G.; Wilson, W. D. *Biochemistry* **1994**, *33*, 5298.
- (63) Lesnik, E. A.; Freier, S. M. *Biochemistry* **1995**, *34*, 10807.
- (64) Clark, C. L.; Cecil, P. K.; Singh, D.; Gray, D. M. *Nucleic Acids Res.* **1997**, *25*, 4098.
- (65) Venkiteswaran, S.; Vijayanathan, V.; Shirahata, A.; Thomas, T.; Thomas, T. J. *Biochemistry* **2005**, *44*, 303.
- (66) Hung, S. H.; Yu, Q.; Gray, D. M.; Ratliff, R. L. *Nucleic Acids Res.* **1994**, *22*, 4326.
- (67) Kankia, B. I.; Marky, L. A. *J. Phys. Chem. B* **1999**, *103*, 8759.
- (68) Freier, S. M.; Kierzek, R.; Jaeger, J. A.; Sugimoto, N.; Caruthers, M. H.; Neilson, T.; Turner, D. H. *Proc. Natl. Acad. Sci. U.S.A.* **1986**, *83*, 9373.
- (69) Huang, Y.; Chen, C.; Russu, I. M. *Biochemistry* **2009**, *48*, 3988.
- (70) Rees, W. A.; Yager, T. D.; Korte, J.; von Hippel, P. H. *Biochemistry* **1993**, *32*, 137.
- (71) Rozners, E.; Moulder, J. *Nucleic Acids Res.* **2004**, *32*, 248.
- (72) Gyi, J. I.; Conn, G. L.; Lane, A. N.; Brown, T. *Biochemistry* **1996**, *35*, 12538.
- (73) Noy, A.; Perez, A.; Marquez, M.; Luque, F. J.; Orozco, M. *J. Am. Chem. Soc.* **2005**, *127*, 4910.
- (74) Priyakumar, U. D.; Mackerell, A. D., Jr. *J. Phys. Chem. B* **2008**, *112*, 1515.
- (75) Zhao, C.; Ren, J.; Qu, X. *Chemistry* **2008**, *14*, 5435.
- (76) Miller, M. C.; Buscaglia, R.; Chaires, J. B.; Lane, A. N.; Trent, J. O. *J. Am. Chem. Soc.* **2010**, *132*, 17105.
- (77) Heddi, B.; Phan, A. T. *J. Am. Chem. Soc.* **2011**, *133*, 9824.
- (78) Hansel, R.; Lohr, F.; Foldynova-Trantirkova, S.; Bamberg, E.; Trantirek, L.; Dotsch, V. *Nucleic Acids Res.* **2011**, *39*, 5768.

- (79) Nakano, S.; Wu, L.; Oka, H.; Karimata, H. T.; Kirihata, T.; Sato, Y.; Fujii, S.; Sakai, H.; Kuwahara, M.; Sawai, H.; Sugimoto, N. *Mol. Biosyst.* **2008**, *4*, 579.
- (80) Minton, A. P. *Biophys. J.* **2005**, *88*, 971.
- (81) Zhou, H. X.; Rivas, G.; Minton, A. P. *Annu. Rev. Biophys.* **2008**, *37*, 375.
- (82) Kilburn, D.; Roh, J. H.; Guo, L.; Briber, R. M.; Woodson, S. A. *J. Am. Chem. Soc.* **2010**, *132*, 8690.
- (83) Spink, C. H.; Chaires, J. B. *Biochemistry* **1999**, *38*, 496.
- (84) Pincus, D. L.; Hyeon, C.; Thirumalai, D. *J. Am. Chem. Soc.* **2008**, *130*, 7364.
- (85) Noy, A.; Luque, F. J.; Orozco, M. *J. Am. Chem. Soc.* **2008**, *130*, 3486.
- (86) Oda, Y.; Iwai, S.; Ohtsuka, E.; Ishikawa, M.; Ikehara, M.; Nakamura, H. *Nucleic Acids Res.* **1993**, *21*, 4690.
- (87) Cerritelli, S. M.; Crouch, R. J. *FEBS J.* **2009**, *276*, 1494.
- (88) Li, F.; Sarkhel, S.; Wilds, C. J.; Wawrzak, Z.; Prakash, T. P.; Manoharan, M.; Egli, M. *Biochemistry* **2006**, *45*, 4141.
- (89) Lener, D.; Kvaratskhelia, M.; Le Grice, S. F. *J. Biol. Chem.* **2003**, *278*, 26526.
- (90) Rausch, J. W.; Qu, J.; Yi-Brunozzi, H. Y.; Kool, E. T.; Le Grice, S. F. *Proc. Natl. Acad. Sci. U.S.A.* **2003**, *100*, 11279.
- (91) Dash, C.; Yi-Brunozzi, H. Y.; Le Grice, S. F. *J. Biol. Chem.* **2004**, *279*, 37095.
- (92) Place, R. F.; Noonan, E. J.; Foldes-Papp, Z.; Li, L. C. *Curr. Pharm. Biotechnol.* **2010**, *11*, 518.
- (93) Kawashima, T.; Amano, N.; Koike, H.; Makino, S.; Higuchi, S.; Kawashima-Ohya, Y.; Watanabe, K.; Yamazaki, M.; Kanehori, K.; Kawamoto, T.; Nunoshiba, T.; Yamamoto, Y.; Aramaki, H.; Makino, K.; Suzuki, M. *Proc. Natl. Acad. Sci. U.S.A.* **2000**, *97*, 14257.
- (94) Nagatoishi, S.; Tanaka, Y.; Kudou, M.; Tsumoto, K. *Mol. Biosyst.* **2010**, *6*, 98.